



Published in final edited form as:

*J Immunol.* 2019 May 01; 202(9): 2661–2670. doi:10.4049/jimmunol.1801118.

## Dragotcytosis: Elucidation of the Mechanism for *Cryptococcus neoformans* Macrophage-to-Macrophage Transfer

Quigly Dragotakes<sup>\*</sup>, Man Shun Fu<sup>\*</sup>, and Arturo Casadevall<sup>\*</sup>

<sup>\*</sup>Department of Molecular Microbiology and Immunology, Johns Hopkins Bloomberg School of Public Health, Baltimore, USA

### Abstract

*Cryptococcus neoformans* is a pathogenic yeast capable of a unique and intriguing form of cell-to-cell transfer between macrophage cells. The mechanism for cell-to-cell transfer is not understood. Here we imaged mouse macrophages with CellTracker Green CMFDA-labeled cytosol to ascertain whether cytosol was shared between donor and acceptor macrophages. Analysis of several transfer events detected no transfer of cytosol from donor to acceptor mouse macrophages. However, blocking Fc and complement receptors resulted in a major diminution of cell-to-cell transfer events. The timing cell-to-cell transfer (11.17 min) closely approximated the sum of phagocytosis (4.18 min) and exocytosis (6.71 min) times. We propose that macrophage cell-to-cell transfer represents a non-lytic exocytosis event followed by phagocytosis into a macrophage that is in close proximity and name this process Dragotcytosis (Dragot is a Greek surname meaning ‘Sentinel’) as it represents sharing of a microbe between two sentinel cells of the innate immune system.

### Introduction

*Cryptococcus neoformans* is a pathogenic fungus that is the causative agent of cryptococcosis, a disease that affects primarily immunocompromised individuals. *C. neoformans* is a facultative intracellular pathogen that infects and reproduces inside of macrophages. Hence, the macrophage is a key cell in the pathogenesis of cryptococcosis and the outcome of the *C. neoformans*-macrophage interaction can determine the outcome of the infection(1–5). The cryptococcal pathogenic strategy is remarkable in that it involves fungal cell survival in a mature phagosome and the phenomenon of non-lytic exocytosis (or Vomocytosis), which is characterized by expulsion of the fungal cells from the macrophage with the survival of both cells(6–8). In addition, *C. neoformans* is capable of being transferred from an infected to a non-infected macrophage(7, 8). Cell-to-cell transfer is generally believed to be a process different from non-lytic exocytosis, with these two events being referred to as Type III and Type II exocytosis, respectively(9), denoting the fact that all

Address Correspondence: Quigly Dragotakes (qdragot@jhu.edu), Phone: 410-955-3457, Fax: 410-955-0105, Johns Hopkins Bloomberg School of Public Health, Department of Molecular Microbiology and Immunology, Baltimore, MD.

<sup>1</sup>The authors declare that we have no commercial or other association which might pose a conflict of interest.

<sup>3</sup>None of the data in this manuscript has been presented at any meetings.

<sup>4</sup>All requests for reprints should be addressed to the corresponding author with information provided on the title page.

<sup>5</sup>No authors affiliations have changed since completion.

these events share in common the exit of a fungal cell from an infected macrophage. Non-lytic exocytosis has been described in mammalian(7, 8), fish(10), insect(11), and amoeba(12) cells and appears to be a highly conserved strategy for *C. neoformans* cells to escape host and environmental predatory phagocytic cells. Non-lytic exocytosis has been described in other pathogenic microbes, including *Burkholderia cenocepacia*(13), *Candida albicans*(14), and *Mycobacterium tuberculosis*(15), suggesting that it may be a widespread strategy for microbial escape from phagocytic cells.

Little is known about the mechanism of cell-to-cell transfer, which could facilitate the spread of infection in anatomical sites where macrophages are in close apposition to one another, such as cryptococcal granulomas and infected lymph nodes. Macrophage to endothelial cell transfer of *C. neoformans* was described in blood-brain barrier models(16). Whether cell-to-cell transfer favors control of infection, or promotes it, it is likely to depend on the circumstances of the host-microbe interaction. For example, transfer of a single fungal cell between two macrophages would appear to be a debit for the host, since *C. neoformans* residence in macrophages is associated with host cell damage(17) and thus could damage two host cells. Conversely, transfer of fungal cells from a macrophage infected with many yeasts could help in the control of infection since it would reduce the multiplicity of infection per cell.

*C. neoformans* cell-to-cell transfer has received relatively little attention, largely because it is difficult to study. We investigated the mechanism of macrophage-to-macrophage transfer of *C. neoformans* cells and found that it involves a coordinated non-lytic exocytosis event from one cell followed by immediate phagocytosis by an adjacent cell. The results implicate non-lytic exocytosis in cell-to-cell transfer.

## Materials and Methods

### C. neoformans Strain and Culture Conditions

Cryptococcal cultures were prepared by inoculating 10 mL Sabouraud Dextrose Broth [SAB; Becton-Dickenson, Franklin Lakes, NJ] media with a stab of frozen *C. neoformans* var. *grubii* serotype A strain H99 stock. Cultures were incubated at 30 °C shaking at 150 rpm for 2 d before use in infections. Cultures were heat killed by incubating for 1 h at 60 °C in a water bath.

### Macrophage culture

Bone-marrow derived macrophages (BMDM) were generated from hind leg bones of 5- to 8-wk-old co-housed C57BL/6 female mice (Jackson Laboratories, Bar Harbor, ME) or Fc receptor knockout (Fcer1g) mice (Taconic model 583) of the same age. For the macrophage differentiation, cells were seeded in 100 mm tissue culture-treated cell culture dishes (Corning, Corning, NY) in Dulbecco's Modified Eagle medium (DMEM; Corning) with 20 % L-929 cell-conditioned medium, 10 % FBS (Atlanta Biologicals, Flowery Branch, GA), 2mM Glutamax (Gibco, Gaithersburg MD), 1 % nonessential amino acid [Cellgro], 1 % HEPES buffer [Corning], 1 % penicillin-streptomycin [Corning] and 0.1 % 2-mercaptoethanol [Gibco] for 6-7 d at 37 °C with 9.5 % CO<sub>2</sub>. Fresh media in 3 ml were

supplemented on day 3 and the medium were replaced on day 6. Differentiated BMDM were used for experiments within 5 days after completed differentiation.

Murine macrophage-like J774.16 cells were maintained in DMEM with 10 % NCTC109 medium [Gibco], 10 % FBS, 1 % nonessential amino acid, 1 % penicillin-streptomycin at 37 °C with 9.5% CO<sub>2</sub>. All murine work was done using protocols reviewed and approved by IACUC. All experimental work in this study was done with BMDM except for the high-resolution movie shown in Figure S1, which was filmed using J774.16 cells.

### Acquisition of Supplemental Video

J774.16 cells were seeded ( $5 \times 10^4$  cells/well) on poly-D-lysine coated coverslip bottom MatTek petri dishes with 14mm microwell [MatTek Brand Corporation] in medium containing 0.5 µg/ml lipopolysaccharide [LPS; Sigma], 0.02 µg/mL (100 U/ml) gamma interferon [IFN $\gamma$ ; Roche]. Cells were then incubated at 37 °C with 9.5 % CO<sub>2</sub> overnight. On the following day, macrophages were infected with cryptococcal cells ( $1.5 \times 10^5$  cells/well) in the presence of 10 µg/ml monoclonal antibody (mAb) 18b7. After 2 h incubation to allow phagocytosis, culture was washed five times with fresh medium to remove extracellular cryptococcal cells. Images were taken every 4 min for 24 h using a Carl Zeiss LSM 780 confocal microscope with a 40 × 1.4 NA Plan Apochromat oil-immersion DIC objective and a spectral GaAsP detector in an enclosed chamber under conditions of 5.0 % CO<sub>2</sub> and 37 °C. Acquisition parameters, shutters and focus were controlled by Zen black software [Carl Zeiss].

### Macrophage Infections and Videos for Cytosol Exchange and Inhibitor Trials

BMDMs were seeded ( $2.5 \times 10^4$  cells/well) in MatTek dishes and 24-well plates [Corning]. Cells in one MatTek dish and one well from the 24-well plate were activated overnight (16h) with IFN $\gamma$  (0.02 µg/mL) and (0.5 µg) LPS. Cells in the MatTek dish were stained with CellTracker Green CMFDA [ThermoFisher] according to manufacturer's protocol before infecting with Uvitex 2B (5 µm/mL ; Polysciences Inc., Warrington, PA) labeled and 18B7 (Generated in lab; 10 µg/mL) or guinea pig complement (20% ; MilliPore) opsonized *Cryptococcus* at an MOI of 1 for 1 h. Cells from the 24-well plate were labeled with CellMask Orange [ThermoFisher] according to manufacturer's protocol, then raised and seeded over the MatTek dish after washing with 2mL fresh cell media three times to reduce extracellular cryptococcal cells. Inspection of MatTek monolayers immediately after washing and before starting the experiments revealed no extracellular *C. neoformans*. Cells were incubated for 30 additional minutes to allow for adhesion before supplementing the plate with 2 mL fresh cell media. MatTek dishes were then placed under a Zeiss axiovert 200M 10X magnification, incubated at 37 °C and 9.5% CO<sub>2</sub>, and imaged every 2 min for a 24 h period. Images were then manually analyzed to identify clear transfer events. For each transfer event donor and acceptor cells were outlined according to cell membranes visible in phase contrast. CellTracker and Uvitex 2B channel intensities were then collected for each pixel within the cell outline and compared using unpaired two-tailed t tests between pre and post transfer quantifications.

Receptor inhibitor experiments used a single MatTek dish with  $5 \times 10^4$  macrophages activated overnight with IFN $\gamma$  (0.02  $\mu\text{g}/\text{mL}$ ) and LPS (0.5  $\mu\text{g}/\text{mL}$ ). Cells were infected with *C. neoformans* at an MOI of 1 for 1 h followed by three washes of 2 mL fresh media to reduce extracellular cryptococcal cells. Cells were incubated for 1h with aCD16/32 anti-Fc receptor antibodies (0.5  $\mu\text{g}/\text{mL}$ ; BD Biosciences 553142) and anti-CD11b antibodies (0.5  $\mu\text{g}/\text{mL}$ ; BD Biosciences 553308) or Cytochalasin B (2, 4, or 10  $\mu\text{M}$ ; Sigma C6762), or Cytochalasin D (2 or 4  $\mu\text{M}$ ; Sigma C8273) before beginning 24 h imaging under the Zeiss axiovert 200M 10X magnification at 37 °C with 9.5 % CO<sub>2</sub> overnight to analyze total cellular exit events.

Fc receptor knockout experiments used a single MatTek dish with  $5 \times 10^4$  macrophages activated overnight with IFN $\gamma$  (0.02  $\mu\text{g}/\text{mL}$ ) and LPS (0.5  $\mu\text{g}/\text{mL}$ ). Cells were infected with *C. neoformans* at an MOI of 1 for 1 h followed by three washes of 2 mL fresh media to reduce extracellular cryptococcal cells. Cells were then imaged for 24 h under the Zeiss axiovert 200M 10X magnification at 37 °C with 9.5 % CO<sub>2</sub> overnight to analyze total cellular exit events. For inhibitor trials, cells were incubated for 1h with CD11b anti-complement antibodies (0.5  $\mu\text{g}/\text{mL}$ ) before beginning 24 h imaging under the Zeiss axiovert 200M 10X magnification at 37 °C with 9.5 % CO<sub>2</sub> overnight to analyze total cellular exit events.

Phagocytosis and non-lytic exocytosis timing experiments were set up as above except using an MOI of 1 for 2 h at 4 °C, then MatTek dishes were placed on the microscope stage, and images were immediately taken every 1 min for 24 h immediately after adding mAb 18B7 (10  $\mu\text{g}/\text{mL}$ ) directly to the dish.

For experiments in which we explored dye acquisition during exposure to the extracellular environment, BMDMs were seeded in a single MatTek dish with  $5 \times 10^4$  macrophages activated overnight with IFN $\gamma$  and LPS. Cells were infected with *C. neoformans* at an MOI of 3 for 1 h followed by three washes of 2 mL fresh media to reduce extracellular cryptococcal cells. Uvitex (50  $\mu\text{m}/\text{mL}$ ) and 18B7 conjugated to Oregon Green (100  $\mu\text{g}/\text{mL}$ ) was supplemented to the extracellular media. Cells were then imaged for 24 h under the Zeiss axiovert 200M 10X magnification at 37 °C with 9.5 % CO<sub>2</sub> overnight to analyze cryptococcal cell acquisition of each dye.

### **BMDM mRNA Gene Expression Array**

BMDMs were seeded in 6-well dishes at  $10^6$  cells per well. Cells were activated overnight with IFN $\gamma$  and LPS. Cells were then treated for 1 h with or without Fc receptor blocking antibody, or harvested before the incubation for a baseline. Cells were lifted from the dishes, pelleted, and resuspended in TRIzol reagent [ThermoFisher]. The supernatant was then flash frozen and stored at -80 °C.

Total RNA was extracted using a PureLink RNA minikit (Ambion/Life Technologies) according to the manufacturer's protocol, including on-column DNase treatment. Following elution of purified RNA from the PureLink columns with nuclease-free water, quantitation was performed using a NanoDrop spectrophotometer, and quality assessment was determined by RNA LabChip analysis on an Agilent Bioanalyzer 2100 system or with RNA

Screen tape on an Agilent TapeStation 2200 system. One hundred nanograms of total RNA was processed for hybridization to Agilent SurePrint G3 mouse (v2) 8×60K gene expression arrays according to Agilent's one-color microarray-based analysis (low-input QuickAmp labeling) protocol, including cDNA synthesis, cRNA synthesis with Cy3 labeling and purification, fragmentation, hybridization, and post-hybridization washing. Spike-In controls were utilized and processed according to Agilent's one-color RNA Spike-In kit protocol. The arrays were scanned in an Agilent G2600D SureScan microarray scanner using scan protocol AgilentG3\_GX\_1color. Agilent's Feature Extraction software was used to assign grids, provide raw image files per array, and generate quality control (QC) metric reports from the microarray scan data. The QC metric reports were used for quality assessment of all hybridizations and scans. Txt files from the Feature Extraction software were imported into the Partek Genomics Suite (v7.0; Partek) for detailed analyses of gene expression. Within Partek, the gProcessedSignal was imported and the intensity values were normalized to the 75th percentile, lower expressed genes were filtered out, and log transformation base 2.0 was performed. The batch effect removal tool (analysis of variance [ANOVA]) was used to correct for effects of array (slide). A two-way ANOVA with linear contrasts for treatment (Antibody) and time (1hr) versus the control (No Antibody 1hr or No Antibody 0hr) was performed with outputs of *P* value, fold change, and mean ratio. The cutoff criteria for filtering gene lists were significant *P* values ( $P < 0.05$ ) with the fold changes of greater than 2 or less than -2. Heatmaps were generated from the filtered gene lists, as well as lists from Venn diagram comparisons. Microarray data has been deposited to the NCBI Gene Expression Omnibus (GEO) repository (GEO dataset # GSE126977) <https://www.ncbi.nlm.nih.gov/geo/query/acc.cgi?acc=GSE126977>.

### Quantification of Temporal Kinetics

Each type of event (phagocytosis, non-lytic exocytosis, and cell-to-cell transfer) was given a start and end based on the movie frame when beginning and ending was observed. The total number of frames spanning from start to end were counted to estimate the duration of the event. The start of phagocytosis was defined as the first frame in which a cryptococcal cell was attached to a macrophage cell, no longer free moving through the media. The end of phagocytosis was defined as the first frame in which it is undeniably clear that the cryptococcal cell has been fully engulfed and is no longer touching the plasma membrane. The start of non-lytic exocytosis was defined as the frame immediately prior to a cryptococcal cell within a macrophage moving toward the plasma membrane. The end of non-lytic exocytosis was defined as the frame in which that cryptococcal cell is fully outside of its host macrophage and no longer in contact with the plasma membrane. The start of a cell-to-cell transfer event was defined in the same way as non-lytic exocytosis, that is the frame immediately prior to movement toward the plasma membrane. The end of a cell-to-cell transfer event was defined in the same way as phagocytosis, that is the frame in which the cryptococcal cell is fully engulfed by the acceptor macrophage and is no longer in contact with the plasma membrane.

### C. neoformans Inhibition Assay

BMDMs were seeded ( $1 \times 10^6$  cells/well) in 6-well tissue culture treated plates [Corning]. Cells in one MatTek dish and one well from the 24-well plate were activated overnight (16

h) with IFN $\gamma$  (0.02  $\mu\text{g}/\text{mL}$ ) and (0.5  $\mu\text{g}$ ) LPS. Cells were then infected with *C. neoformans* opsonized with 18B7 (10  $\mu\text{g}/\mu\text{L}$ ) at MOI 3 and incubated a further 24 h. Wells were washed twice with 1 mL HBSS then lifted with CellStripper and pelleted via centrifugation (350  $\times$  g for 10 min). Macrophages were then lysed via resuspension in 500  $\mu\text{L}$  dH $_2\text{O}$  for 10 min. Released *C. neoformans* were then plated on a SAB agar plate in a serial dilution of 8  $\times$  1/3 dilutions. SAB agar plates were incubated at 30  $^{\circ}\text{C}$  for 2 d. To quantify, the smallest dilution with at least 1 colony was identified for each sample. Colony counts were back calculated to the highest common dilution and compared.

## Statistics

Statistical differences between dye channels for both cytosolic (CellTracker Green) and cryptococcal (Uvitex 2B) were determined by two-tailed unpaired t-test between cells pre and post transfer. The region of interest was manually defined by the exterior of the host cell plasma membrane via phase contrast channel. Each pixel within the designated region was measured for intensity in its respective channel. Graphs are a depiction of pixel intensity values with bars representing minimum and maximum values. Statistics were calculated on these groups of pixel intensity values. For inhibitor trials significance was calculated using a one-sided test of proportions for each condition compared to the control (18B7 opsonized with no inhibiting antibody treatment).

## Results

### High Resolution Imaging of Cell-to-Cell Transfer

Cryptococcal cell-to-cell transfer was observed by imaging *J774.16* cells infected with *C. neoformans* overnight with phase contrast microscopy (SMovie 1). The coordination apparently involved in this event suggests an underlying mechanism involving both the donor and acceptor cell.

### Cytosol Transfer was not Detected During Cryptococcal Transfer

To determine whether cytosol was transferred from donor to acceptor cell along with *Cryptococcus* cells during fungal macrophage-to-macrophage cell transfer, we visualized transfer events in which only the donor cell was stained with a permanent cytosolic dye in BMDMs. BMDMs were used in this and all proceeding experiments described in this manuscript. Upon identifying a transfer event the microscopic images were isolated before, during, and after the transfer event (Figure 1). This experiment was repeated until ten independent events were identified and the individual fluorescent channels were quantified at each frame before and after Cryptococcal cell transfer. We ensured donor (positive) and acceptor (negative) cell populations were distinguishable by cytoplasmic stain intensity, even at the upper dynamic range of the assay (SFig 1). We found that cytosolic dye signal remained constant in the donor (Figure 2A) and was not observable above background in the acceptor (Figure 2B) cell throughout the event. However, fluorescence intensity corresponding to cryptococcal cells decreased in the donor cell (Figure 2C) and increased in the acceptor cell (Figure 2D) after transfer. This analysis was repeated for every event. Taken together these data showed no evidence that host cell cytosol was transferred during cryptococcal cell-to-cell transfer. Additionally, we performed experiments supplemented

with a plasma membrane stain (CellMask Orange; ThermoFisher) and identified two transfer events. There was no intensity difference between plasma membrane staining before and after transfer, suggesting that there is no mixing between donor and acceptor cell plasma membranes during transfer events (SFig 2).

### Cell-to-Cell Transfer Requires FcR and/or Complement Receptor

No cytosolic dye transfer between macrophages during transfer events suggests two hypotheses: 1. Cryptococcal cells are transferred via coordinated exocytosis followed by phagocytosis between the two macrophages; or 2. Only the phagosome is directly transferred between macrophages in a manner that excludes cytosol. Given that the *C. neoformans* capsule prevents phagocytosis(18, 19), that opsonin is required for ingestion(20), and that capsule-associated antibody is present after exocytosis(21), we designed experiments to test the first hypothesis. Specifically, we investigated whether cell-to-cell transfer was blocked by the addition of an anti-CD16/32 monoclonal antibody, which prevents FcR function, in BMDMs. Transfer events were drastically reduced by blocking the FcR but interestingly, occasional cell transfer events were still observed. Additionally, lytic and non-lytic exocytosis events were both unexpectedly reduced in anti-CD16/32 incubated BMDMs compared to control. It is known that opsonized cryptococcal cells can be phagocytosed via complement receptor (CR) by a mechanism where antibody modifies the capsule and allows direct interaction with this receptor in the absence of complement(22). To investigate whether this was the case, the experiments were repeated with complement inhibiting antibody (anti-CD11b) and both inhibiting antibodies. The frequency of cell-to-cell transfer was significantly reduced compared to control when each of the FcR and CR were inhibited and completely abrogated when both were inhibited together, with  $P < 0.01$ , 0.05, and 0.001, respectively (Figure 3A, Table I).

To investigate whether the reduction in observed effects was a consequence of antibody incubation we extracted RNA from BMDMs incubated with or without the Fc receptor blocking antibody and analyzed mRNA gene expression levels between the cells. We found that no genes were significantly differentially regulated with an FDR threshold of 0.05, and only 10 uniquely significantly differentially regulated genes when the cutoff was loosened to an unadjusted  $P$  value  $< 0.05$  (Table II). The data suggests incubation of BMDMs with receptor blocking antibodies had no significant effect on the transcriptional profile relative to cells and thus the reduction in transfer events measured is not likely to be due to an effect of the antibody itself on the host macrophage.

To further explore this phenomenon, we infected BMDMs harvested from Fc receptor knockout mice (*Fcgr1g*) opsonized with 18B7 antibody. We found that *Fcgr1g* BMDMs experienced cell-to-cell transfer significantly less than the control,  $P < 0.01$ , and at a similar rate as wild-type cells incubated with the anti-FcR antibody (Figure 3A, Table I). These data suggested that both Fc and complement receptor mediated phagocytosis can be utilized in cell-to-cell transfer.

We hypothesized that the initial phagocytic event may have downstream effects on whether Cryptococcal cells can undergo cell-to-cell transfer. To explore a potential effect of complement mediated phagocytosis, we repeated these experiments with guinea pig

complement opsonized *C. neoformans* on wild type BMDMs. We found that BMDMs which had ingested *C. neoformans* via complement experienced abrogated cell-to-cell transfer compared to control and in frequencies similar to both wild-type BMDMs inhibited with anti-FcR antibodies and Fc $\gamma$ 1g BMDMs with no inhibiting antibodies (Figure 3A, Table I).

Finally, we also performed experiments supplemented with cytochalasin B, an actin inhibitor, reasoning that actin activity is required for exocytosis. We observed no transfer events, with  $P < 0.001$  compared to control, further supporting the idea that transfer relies on exocytosis events (Figure 3A, Table I). Interestingly, previous reports suggested that transfer events were inhibited(7) but non-lytic exocytosis events were present(23) or even increased(6) with cytochalasin D treatment at low concentrations, 4  $\mu$ M and 2  $\mu$ M in J774 cells. In both cases, however, this was simply a noted observation without in depth experimental analysis. Additionally, in these cases non-lytic exocytosis events were observed almost immediately after adding cytochalasin D, 3-5 min, whereas our experiments included a 1 h incubation with cytochalasin B before starting image acquisition. Additionally, these experiments used different host cells and/or *C. neoformans* strains. We therefore sought to replicate these experimental conditions utilizing our primary BMDM cells. Surprisingly, treating BMDMs with 4  $\mu$ M cytochalasin D resulted in the formation of extremely large, bulbous, vacuole-like organelles around cryptococcal cells (SFig 3). These formations would sometimes rupture, leading to lysis of the host macrophage. Regardless, we observed neither transfer events nor non-lytic exocytosis events and given these results, we favored the first hypothesis as the continued presence of a phagosome around the cryptococcal cell would block antibody-receptor interactions.

### C. neoformans Cells Must be Alive for Cell-to-Cell Transfer

To determine whether macrophage-to-macrophage transfer is an active process on the part of *C. neoformans*, we infected BMDMs with heat killed *C. neoformans* yeasts opsonized with 18B7. We found no examples of lytic exocytosis, non-lytic exocytosis, or cell-to-cell transfer events when macrophages were infected with heat killed *C. neoformans* (Figure 3A, Table I). Additionally, when macrophages were infected with heat killed *C. neoformans* and treated with cytochalasin D we did not observe the above described bulbous vacuole-like organelle development.

### Temporal Kinetics of Cell-to-Cell Transfer

If Cryptococcal cells are transferred via exocytosis followed by phagocytosis it would follow that the total time of transfer events should resemble the length of exocytosis plus the length of phagocytosis. Cell-to-cell transfer time was estimated by counting the total number of frames immediately prior to immediately after transfer, as each frame represented a set number of minutes progression in time. Each image was taken at two-minute intervals, and so the total time of transfer was directly calculated by the number of frames. We found that the median and mean transfer times were 11 and 11.17 minutes, respectively, from twelve total analyzed events (Figure 3B). To our knowledge the timing of neither phagocytosis nor non-lytic exocytosis of *C. neoformans* by BMDMs has been previously carefully measured. To investigate whether the timing of cell-to-cell transfer matched the times of exocytosis and phagocytosis, we visualized phagocytosis by repeating the infection movie protocol but only



adding opsonizing antibody immediately before starting image acquisition. We observed phagocytic events and counted the number of frames (taken each minute) to determine an experimental estimate of phagocytosis ingestion time. Based on eleven observed phagocytic events we determined ingestion occurred over approximately 4.18 minutes (Figure 3B). We then timed non-lytic exocytosis events. Based on seven observed non-lytic exocytosis events we determined a total expulsion time of approximately 6.71 minutes (Figure 3B). Adding the time required for non-lytic exocytosis (6.71 minutes) to that required for phagocytosis (4.18 minutes) yielded 10.9 minutes, which is tantalizingly close to the measured average time of 11.17 minutes for cell-to-cell transfer,  $P > 0.05$  (Figure 3C). Our measured time for cell-to-cell transfer is close to the 10 minutes reported in the initial description of this phenomenon (8). In fact, the relatively short time involved in cell-to-cell transfer precluded us from using either the cell wall dye (Uvitex 2B) or fluorophore conjugated antibody in to stain *C. neoformans* cells during the brief time that they would presumably be exposed to cytoplasm in an exocytosis-phagocytosis event. The time needed for either Uvitex or antibody cellular staining exceeded the longest observed time for cell-to-cell transfer, requiring an average time of 30 and 65 minutes to gain appreciable signal, respectively (Figure 4). However, we made the interesting observation that incubation of macrophages containing ingested *C. neoformans* led to Uvitex staining of yeast cells in some phagosomes, particularly larger ones containing multiple yeast cells (SFig 4). Whether this reflects some mechanism for leakage of Uvitex into cells or dye transport into the phagosome in a mechanism involving pinocytosis and delivery to phagosome(24), this observation may be worthy of future study.

Additionally, we investigated the amount of time required post-infection for transfer events to start occurring. We found that cell-to-cell transfer events predominantly occur within the first 9 hours of the experiment, with an average initiation time of approximately 6.7 h (Figure 3D).

### Host Macrophages Establish Contact Before Transfer

It was previously reported that host macrophage membranes contact each other before cryptococcal cell-to-cell transfer(9, 25). We investigated this further by investigating each of 38 transfer events for whether the donor and acceptor macrophages appeared to establish membrane contact before transfer. We found that in every situation the donor and acceptor cells came in close proximity at least two minutes (one frame) prior to transfer, remained in contact during transfer, and maintained contact for a short time after transfer as well (Figure 5).

### A Model for Macrophage-to-Macrophage Cellular Transfer

Our results indicate that cell-to-cell transfer is a coordinated process between two macrophages, that it does not involve the transfer of cytosol (e.g. Trogocytosis), and that it does not occur when the opsonic Fc and complement receptors are blocked. The time required for cell-to-cell transfer closely approximates addition of the times required for non-lytic exocytosis and ingestion. Although no single observation provides a mechanism, when our results are considered in combination, the most parsimonious interpretation is that *C.*

*neoformans* cell-to-cell transfer results from sequential non-lytic exocytosis events followed by subsequent phagocytosis of expelled yeast cells by an adjacent macrophage. (Figure 6).

### **Blockading Fc and Complement Receptors Leads to Increased *C. neoformans* Intracellular Inhibition**

To investigate the potential physiological relevance of this phenomenon, we decided to quantify and compare the ability of receptor blocked BMDMs to kill ingested *C. neoformans*. BMDMs were seeded, activated, and infected for a 24 h interval supplemented with Fc receptor inhibitory antibodies, both Fc and C receptor inhibitory antibodies, or simply additional cell media. When surviving intracellular *C. neoformans* were quantified we found reduced numbers of viable *C. neoformans* cells when BMDMs were incubated with either Fc or Fc and C receptor inhibitory antibodies (Figure 7). These data support the hypothesis that cryptococcal macrophage-to-macrophage favors pathogen survival and spread.

### **Discussion**

Cell-to-cell transfer was described simultaneously by two independent groups, including our own, in 2007(7, 8). Both groups noted that donor and acceptor cells established contact and that actin was involved at the membrane interface between macrophages. There was speculation about membrane fusion as a preliminary step in cell-to-cell transfer, but this was never experimentally established. Little progress has been made in unraveling the mechanism primarily because cell-to-cell transfer events are relatively rare, occurring sporadically and unpredictably. In fact, the mechanism by which a fungal cell transfers between intact macrophages has been difficult to envision given that it would involve a yeast cell in a membrane-bound phagosome crossing two plasma membranes.

We considered several hypotheses for the mechanism of cryptococcal cell-to-cell transfer. Initially we were intrigued by the possibility that transfer occurred via Trogocytosis, a cellular communication process in which cytosol and surface proteins are shared between macrophages(27). Trogocytosis was previously shown to be a mechanism that intracellular pathogens can utilize and promote to spread between macrophage cells(28). However, when we labeled the cytosol of cryptococcus-infected macrophages we detected no cytosol transfer from donor to acceptor cell during cryptococcal transfer. It should be noted that the shift in Uvitex 2B signal is immediately apparent despite the Uvitex 2B positive population (corresponding to the cryptococcal cell) accounting for a particularly small subset of the entire region of interest. Therefore, even a small amount of dye transferred to the donor cell would noticeably shift the distribution post-transfer. Similarly, we detected no transfer of plasma membrane between macrophages in the experiments supplemented with membrane dye. Obviously, one cannot rule out that an iota of cytosol transferred since that would involve proving a negative, but the absence of any signal indicating cytosol transfer is strong evidence against a mechanism involving a cell-to-cell channel or bridge where donor and acceptor cytoplasm contact. These experiments essentially rule out Trogocytosis as the mechanism of cryptococcal cell-to-cell transfer.

Next, we investigated whether cell-to-cell transfer was a non-lytic exocytosis event followed by ingestion of the expelled yeast by a proximal macrophage. Supporting this hypothesis was the observation that expelled yeast cells have residual opsonizing antibody bound to their capsule even after phagosomal residence, which could support subsequent phagocytosis(21). When both Fc receptor (FcR) and complement receptor (CR) were blocked no transfer events were observed. Although our conditions did not contain complement-derived opsonin, antibody binding to *C. neoformans* capsule results in structural changes that allow complement-independent phagocytosis via complement receptor(22). The measured length of transfer also supports the exocytosis-phagocytosis hypothesis. We determined the average length of non-lytic exocytosis events to be approximately 7 min, consistent with the prior reported 4-12 min(31). Macrophage phagocytosis of *C. neoformans* took approximately 4 min. Last, we found that complete transfer required approximately 11 min, close to the time required for both phagocytosis and non-lytic exocytosis of *C. neoformans*. These observations imply that cell-to-cell transfer is a sequential non-lytic exocytosis event followed by immediate phagocytosis by a nearby macrophage.

When macrophages were incubated with FcR and CR blocking antibodies non-lytic exocytosis events were reduced, but not completely abrogated, compared to controls. This finding suggests that receptor blocking also affects exocytosis, raising the possibility that reduced transfer in the presence of blocking antibody is a consequence of fewer potential donor cells. Consequently, we performed a microarray experiment comparing the transcriptome of macrophages treated with blocking antibody to a control population and were unable to detect significant differences. In addition, we analyzed cell-to-cell transfer using FcR knockout mice macrophages. As previously noted, opsonizing *C. neoformans* with 18B7 allows phagocytosis via CR so these macrophages can still be infected are unable to undergo cell-to-cell transfer via FcR. As hypothesized, transfer events in FcR knockout mice were reduced to levels similar to macrophages inhibited via FcR blockading antibody, while lytic and non-lytic events were not significantly reduced compared to wild type macrophages.

Based on the incomplete inhibition of transfer events with only FcR inhibited, we decided to investigate the contribution of CR, hypothesizing that it could be an alternative, less efficient cell-to-cell transfer route. Wild-type macrophages infected with guinea pig complement opsonized *C. neoformans* experienced transfer rates similar to wild-type macrophages inhibited with anti-FcR antibody and macrophages from FcR knockout mice, while neither lytic nor non-lytic exocytosis events were significantly reduced compared to control. These data support our overall hypothesis that transfer is a coordinated event of non-lytic exocytosis followed by phagocytosis. Transfer can be achieved through either FcR or CR mediated phagocytosis, though FcR mediated phagocytosis is more efficient and common.

To determine if inhibiting actin polymerization affects transfer frequency, we repeated these experiments with cytochalasin-treated macrophages. We hypothesized that if actin was required to expel cryptococcal cells, then its inhibition would result in fewer transfers. Our data supported this hypothesis but differs from a previous report(6) in which transfer increased after cytochalasin treatment. We tried to reproduce those findings and were unable

to identify the source of the discrepancy, although it is possibly due to the use of different types of host cells. Finally, we attempted to show that fungal cells enter the extracellular environment by adding dyes (Uvitex 2B and antibody conjugated fluorophore) to the media. Unfortunately, the time required for yeasts to acquire staining was longer than the length of transfer. Additionally, Uvitex 2B permeated certain macrophages, yielding stained *C. neoformans* cells which never exited their host cell.

A coordinated exocytosis-phagocytosis mechanism allows us to discard more complex explanations. For example, the publications which discovered cryptococcal cell-to-cell transfer hypothesized that direct “cell-to-cell bridges” formed through merging and subsequent unmerging of host cell membranes, allowing direct transfer of the cryptococcus containing organelle. This explanation was suggested without experimental data and does not explain our results as inhibition of antibody receptors should not inhibit the direct transfer of an organelle. If cryptococcal cells were retained in the phagosome throughout the transfer process, then the phagosomal membrane would separate the opsonized yeast from contact with FcR and CR on the acceptor cell surface. Another hypothesis was that cryptococcal cells are transferred via membrane tunnel structures between macrophages. A tunnel transfer explanation is unlikely given that tunnels were absent from our microscopy analysis. In fact, when tunnels form they are too small for even cytosolic molecules to traverse(29). In any case, a tunnel is also ruled out by the fact that transfer was abrogated by blocking cell surface opsonic receptors. Finally, due to the roles of FcR and CR in immune synapse formation, we contemplated the possibility of cryptococcal transfer between macrophages via some type of uncharacterized, macrophage specific immune synapse but concluded this is also unlikely with respect to the data. Immune synapses allow only small molecules and dyes to directly transfer. Particles larger than 32 nm are entirely excluded(30), which also excludes *C. neoformans*.

We have termed the exocytosis-phagocytosis phenomenon Dragotcytosis, to denote that this is a transfer between two sentinel (Greek ‘Dragot’) phagocytic cells. The coupled exocytosis-phagocytosis phenomenon is a new process in microbe-macrophage interactions and warrants a new name to distinguish it from other mechanisms of cell entrance or exit, such as: Trogocytosis, non-lytic exocytosis, and phagocytosis. Dragotcytosis differs from other mechanisms of cell to cell transfer mainly in that it involves the complete expulsion of yeast cells from one macrophage before engulfment by another. Furthermore, Dragotcytosis differs from a simple sequence of exocytosis and phagocytosis in that the donor and acceptor cell are in physical contact before the event occurs and remain in contact through the process. Whether cell contact is involved in triggering exocytosis is an important question for future studies. Dragotcytosis is anticipated to occur in other pathogenic microbes capable of triggering exocytosis such as *Candida albicans*(14), *Mycobacteria tuberculosis*(32), *Serratia marcescens*(33), provided opsonins are available.

The experiments here do not directly address the biological significance of Dragotcytosis. In fact, designing an experiment to assess biological significance by interfering with Dragotcytosis then measuring an outcome related to cryptococcal infection is not possible without introducing a variety of downstream changes that would raise serious doubts about any association between measured effects on virulence and this process. To interfere with

Dragotcytosis *in vivo* would require preventing either phagocytosis or non-lytic exocytosis and such interference would have important secondary effects on host defense and intracellular pathogenesis, respectively. Instead, we argue for the significance of this effect from logical inference and deduction. Phagocytosis is a fundamental cellular host defense mechanism that occurs *in vivo* during cryptococcal infection, evident from the intracellular residence of cryptococci during infection(3, 4). Non-lytic exocytosis is a complex cellular process shown to occur during cryptococcal infection in mice, zebra fish, and amoeba (12, 34, 35). Hence, both phagocytosis and non-lytic exocytosis occur both *in vivo* and *in vitro* (3, 35). During cryptococcal infection, yeast reside in granulomatous inflammation where the cellular density of macrophages is much greater than the *in vitro* conditions where Dragotcytosis was shown to occur in this study (3). Given the occurrence of its component processes of phagocytosis and non-lytic exocytosis *in vivo* and that *C. neoformans* often resides in granulomas where macrophages exist in close apposition, it is likely that Dragotcytosis occurs *in vivo*.

Dragotcytosis may result in an overall benefit to *C. neoformans* rather than the host. After infecting BMDMs with *C. neoformans*, we found that inhibiting Dragotcytosis through blocking FcR and CR reduced *C. neoformans* viability. This suggests that the ability of *C. neoformans* to freely move between macrophages is advantageous to the yeast. We considered the possibility that addition of blocking antibodies was activating the macrophages in some way to enhance their antifungal activity but found no evidence that receptor blockage affected transcriptional responses. We know *C. neoformans* can reside in macrophages for hours, if not days, and it is possible that antifungal effects in phagolysosomes take time to be effective in inhibiting fungal replication. Hence, moving to a younger phagolysosome by Dragotcytosis could benefit fungal cells. We confirmed that *C. neoformans* viability is essential for non-lytic exocytosis and Dragotcytosis. We recognize that if inhibition of Dragotcytosis enhances antifungal activity, and that fungal viability is needed for exocytosis, the latter alone could reduce the frequency of Dragotcytosis. However, we note non-lytic exocytosis occurs relatively early (< 4 h) in macrophage infection (9) while the commencement of intracellular budding occurs later, peaking at 6-10 h (36). Indeed, we observed the initiation of Dragotcytosis events early in macrophage infection as well (approximately 6.7 h). Hence, although we cannot fully separate reduction in Dragotcytosis by receptor blocking from enhanced inhibition of *C. neoformans* in macrophages where the fungal cell cannot escape, the available data favors a temporal sequence where inhibition of Dragotcytosis is followed by inhibition of fungal replication.

In summary, three lines of evidence strongly suggest that Dragotcytosis represents sequential exocytosis-phagocytosis events: 1) we observed no cytosol transfer from donor to receptor cell; 2) the frequency of transfer events was greatly reduced by interference with phagocytic receptors; and 3) the time involved in Dragotcytosis was indistinguishable from the sum of the times involved in exocytosis and phagocytosis. The implications of Dragotcytosis for pathogenesis and host defense are uncertain and may vary with infection setting. Antibody administration can protect mice against cryptococcal infection(37). Comparative analysis of infected tissues of antibody-treated and control mice shows that presence of antibody is associated with increased *C. neoformans* intracellular residence in macrophages(38), which was interpreted as reflecting more efficient antibody-mediated phagocytosis. However, our

results suggest that Dragotcytosis could contribute to this effect since fungal cells experiencing non-lytic exocytosis in granulomas could be rapidly ingested by proximal macrophages, perpetuating intracellular residence. The dependence on phagocytic receptors and opsonins has the interesting implication that Dragotcytosis may be more frequent in hosts with robust antibody responses. Since non-lytic exocytosis has been described with several other pathogens, Dragotcytosis could theoretically occur in other infections. Whether Dragotcytosis benefits the host by promoting re-ingestion of expelled cells or harms the host by promoting new cellular infections capable of disseminating in a Trojan Horse manner is not known and probably depends on the circumstances when it occurs. Future research into Dragotcytosis should focus on elucidating the factors that control the frequency of transfer and the macrophage and/or fungal signals that trigger this process.

## Supplementary Material

Refer to Web version on PubMed Central for supplementary material.

## Acknowledgements

Quigly Dragotakes would like to acknowledge Gundula Bosch Ph.D, Clive Shiff Ph.D., and David Sullivan M.D. for the timely assignment of a Trogocytosis paper in journal club during his rotation in the Casadevall Lab which inspired him to investigate this phenomenon.

Additionally, we would like to thank Carolina Coelho Ph.D. for sharing BMDM harvesting responsibilities on many occasions and the hard work of Amanda Dziedzic and Anne Jedlicka in the JHSPH Genomic Analysis and Sequencing Core for harvesting mRNAs and running the microarrays.

2. Arturo Casadevall is supported by 5R01HL059842, 5R01AI033774, 5R37AI033142, and 5R01AI052733. Quigly Dragotakes is supported by a T32 and a fellowship from the ARCS-MWC foundation.

## References

1. Johnston SA, and May RC. 2013 *Cryptococcus* interactions with macrophages: evasion and manipulation of the phagosome by a fungal pathogen. *Cell. Microbiol.* 15: 403–411. [PubMed: 23127124]
2. Alanio A, Vernel-Pauillac F, Sturny-Leclère A, and Dromer F. 2015 *Cryptococcus neoformans* host adaptation: toward biological evidence of dormancy. *MBio* 6.
3. Feldmesser M, Kress Y, Novikoff P, and Casadevall A. 2000 *Cryptococcus neoformans* is a facultative intracellular pathogen in murine pulmonary infection. *Infect. Immun.* 68: 4225–4237. [PubMed: 10858240]
4. Levitz SM, Nong SH, Seetoo KF, Harrison TS, Speizer RA, and Simons ER. 1999 *Cryptococcus neoformans* resides in an acidic phagolysosome of human macrophages. *Infect. Immun.* 67: 885–890. [PubMed: 9916104]
5. Davis MJ, Tsang TM, Qiu Y, Dayrit JK, Freij JB, Huffnagle GB, and Olszewski MA. 2013 Macrophage M1/M2 polarization dynamically adapts to changes in cytokine microenvironments in *Cryptococcus neoformans* infection. *MBio* 4: e00264–00213. [PubMed: 23781069]
6. Alvarez M, and Casadevall A. 2006 Phagosome Extrusion and Host-Cell Survival after *Cryptococcus neoformans* Phagocytosis by Macrophages. *Curr. Biol.* 16: 2161–2165. [PubMed: 17084702]
7. Alvarez M, and Casadevall A. 2007 Cell-to-cell spread and massive vacuole formation after *Cryptococcus neoformans* infection of murine macrophages. *BMC Immunol.* 8: 16. [PubMed: 17705844]
8. Ma H, Croudace JE, Lammas DA, and May RC. 2007 Direct cell-to-cell spread of a pathogenic yeast. *BMC Immunol.* 8: 15. [PubMed: 17705831]

9. Stukes SA, Cohen HW, and Casadevall A. 2014 Temporal Kinetics and Quantitative Analysis of *Cryptococcus neoformans* Nonlytic Exocytosis. *Infect. Immun.* 82: 2059–2067. [PubMed: 24595144]
10. Davis JM, Huang M, Botts MR, Hull CM, and Huttenlocher A. 2016 A Zebrafish Model of Cryptococcal Infection Reveals Roles for Macrophages, Endothelial Cells, and Neutrophils in the Establishment and Control of Sustained Fungemia. *Infect. Immun.* 84: 3047–3062. [PubMed: 27481252]
11. Qin Q-M, Luo J, Lin X, Pei J, Li L, Ficht TA, and de Figueiredo P. 2011 Functional analysis of host factors that mediate the intracellular lifestyle of *Cryptococcus neoformans*. *PLoS Pathog.* 7: e1002078. [PubMed: 21698225]
12. Chrisman CJ, Alvarez M, and Casadevall A. 2010 Phagocytosis of *Cryptococcus neoformans* by, and Nonlytic Exocytosis from, *Acanthamoeba castellanii*. *Appl. Environ. Microbiol.* 76: 6056–6062. [PubMed: 20675457]
13. Vergunst AC, Meijer AH, Renshaw SA, and O’Callaghan D. 2010 *Burkholderia cenocepacia* creates an intramacrophage replication niche in zebrafish embryos, followed by bacterial dissemination and establishment of systemic infection. *Infect. Immun.* 78: 1495–1508. [PubMed: 20086083]
14. Bain JM, Lewis LE, Okai B, Quinn J, Gow NAR, and Erwig L-P. 2012 Non-lytic expulsion/exocytosis of *Candida albicans* from macrophages. *Fungal Genet. Biol.* 49: 677–678. [PubMed: 22326419]
15. Hagedorn M, Rohde KH, Russell DG, and Soldati T. 2009 Infection by tubercular mycobacteria is spread by nonlytic ejection from their amoeba hosts. *Science* 323: 1729–1733. [PubMed: 19325115]
16. Santiago-Tirado FH, Onken MD, Cooper JA, Klein RS, and Doering TL. 2017 Trojan Horse Transit Contributes to Blood-Brain Barrier Crossing of a Eukaryotic Pathogen. *MBio* 8.
17. Coelho C, Souza ACO, da S. Derengowski L, de Leon-Rodriguez C, Wang B, Leon-Rivera R, Bocca AL, Gonçalves T, and Casadevall A. 2015 Macrophage mitochondrial and stress response to ingestion of *Cryptococcus neoformans*. *J. Immunol. (Baltimore, Md. 1950)* 194: 2345–2357.
18. Syme RM, Bruno TF, Kozel TR, and Mody CH. 1999 The capsule of *Cryptococcus neoformans* reduces T-lymphocyte proliferation by reducing phagocytosis, which can be restored with anticapsular antibody. *Infect. Immun.* 67: 4620–7. [PubMed: 10456908]
19. Kozel TR, and Gotschlich EC. 1982 The capsule of *cryptococcus neoformans* passively inhibits phagocytosis of the yeast by macrophages. *J. Immunol.* 129: 1675–80. [PubMed: 7050244]
20. Heitman J, Kozel TR, Kwon-Chung K, Perfect J, and Casadevall A. 2011 The Interaction of *Cryptococcus neoformans* with Host Macrophages and Neutrophils. *ASM Press* 373–385.
21. Alvarez M, Saylor C, and Casadevall A. 2008 Antibody action after phagocytosis promotes *Cryptococcus neoformans* and *Cryptococcus gattii* macrophage exocytosis with biofilm-like microcolony formation. *Cell. Microbiol.* 10: 1622–1633. [PubMed: 18384661]
22. Taborda CP, and Casadevall A. 2002 CR3 (CD11b/CD18) and CR4 (CD11c/CD18) are involved in complement-independent antibody-mediated phagocytosis of *Cryptococcus neoformans*. *Immunity* 16: 791–802. [PubMed: 12121661]
23. Ma H, Croudace JE, Lammas DA, and May RC. 2006 Expulsion of Live Pathogenic Yeast by Macrophages. *Curr. Biol.* 16: 2156–2160. [PubMed: 17084701]
24. Edelson BT, and Unanue ER. 2001 Intracellular antibody neutralizes *Listeria* growth. *Immunity* 14: 503–12. [PubMed: 11371353]
25. Alvarez M, and Casadevall A. 2007 Cell-to-cell spread and massive vacuole formation after *Cryptococcus neoformans* infection of murine macrophages. *BMC Immunol.* 8: 16. [PubMed: 17705844]
26. Casadevall A 2010 Cryptococci at the brain gate: break and enter or use a Trojan horse? *J. Clin. Invest.* 120: 1389–1392. [PubMed: 20424319]
27. Joly E, and Hudrisier D. 2003 What is trogocytosis and what is its purpose? *Nat. Immunol.* 4: 815. [PubMed: 12942076]
28. Steele S, Radlinski L, Taft-Benz S, Brunton J, and Kawula TH. 2016 Trogocytosis-associated cell to cell spread of intracellular bacterial pathogens. *Elife* 5: e10625. [PubMed: 26802627]

29. Rustom A, Saffrich R, Markovic I, Walther P, and Gerdes H-H. 2004 Nanotubular Highways for Intercellular Organelle Transport. *Science* (80-. ). 303: 1007–1010.
30. Cartwright ANR, Griggs J, and Davis DM. 2014 The immune synapse clears and excludes molecules above a size threshold. *Nat. Commun.* 5: 5479. [PubMed: 25407222]
31. Stukes S, and Casadevall A. 2014 Visualizing non-lytic exocytosis of *Cryptococcus neoformans* from macrophages using digital light microscopy. *J. Vis. Exp. JoVE* e52084. [PubMed: 25350860]
32. Quigley J, Hughitt VK, Velikovsky CA, Mariuzza RA, El-Sayed NM, and Briken V. 2017 The Cell Wall Lipid PDIM Contributes to Phagosomal Escape and Host Cell Exit of *Mycobacterium tuberculosis*. *MBio* 8.
33. Di Venanzio G, Lazzaro M, Morales ES, Krapf D, and García Vescovi E. 2017 A pore-forming toxin enables *Serratia* a nonlytic egress from host cells. *Cell. Microbiol.* 19: e12656.
34. Bojarczuk A, Miller KA, Hotham R, Lewis A, Ogryzko NV, Kamuyango AA, Frost H, Gibson RH, Stillman E, May RC, Renshaw SA, and Johnston SA. 2016 *Cryptococcus neoformans* Intracellular Proliferation and Capsule Size Determines Early Macrophage Control of Infection. *Sci. Rep.* 6: 21489. [PubMed: 26887656]
35. Nicola AM, Robertson EJ, Albuquerque P, Derengowski L. d. S., and Casadevall A. 2011 Nonlytic Exocytosis of *Cryptococcus neoformans* from Macrophages Occurs In Vivo and Is Influenced by Phagosomal pH. *MBio* 2.
36. Fu MS, Coelho C, De Leon-Rodriguez CM, Rossi DCP, Camacho E, Jung EH, Kulkarni M, and Casadevall A. 2018 *Cryptococcus neoformans* urease affects the outcome of intracellular pathogenesis by modulating phagolysosomal pH. *PLOS Pathog.* 14: e1007144. [PubMed: 29906292]
37. Casadevall A, and Pirofski L-A. 2012 Immunoglobulins in defense, pathogenesis, and therapy of fungal diseases. *Cell Host Microbe* 11: 447–456. [PubMed: 22607798]
38. Feldmesser M, and Casadevall A. 1997 Effect of serum IgG1 to *Cryptococcus neoformans* glucuronoxylomannan on murine pulmonary infection. *J. Immunol. (Baltimore, Md. 1950)* 158: 790–799.



**Key Points**

*C. neoformans* transfer between macrophages in coordinated exocytosis-phagocytosis.

Opsonin receptors are utilized for transfer process.

*C. neoformans* must be viable for transfer process to occur.

Author Manuscript

Author Manuscript

Author Manuscript

Author Manuscript

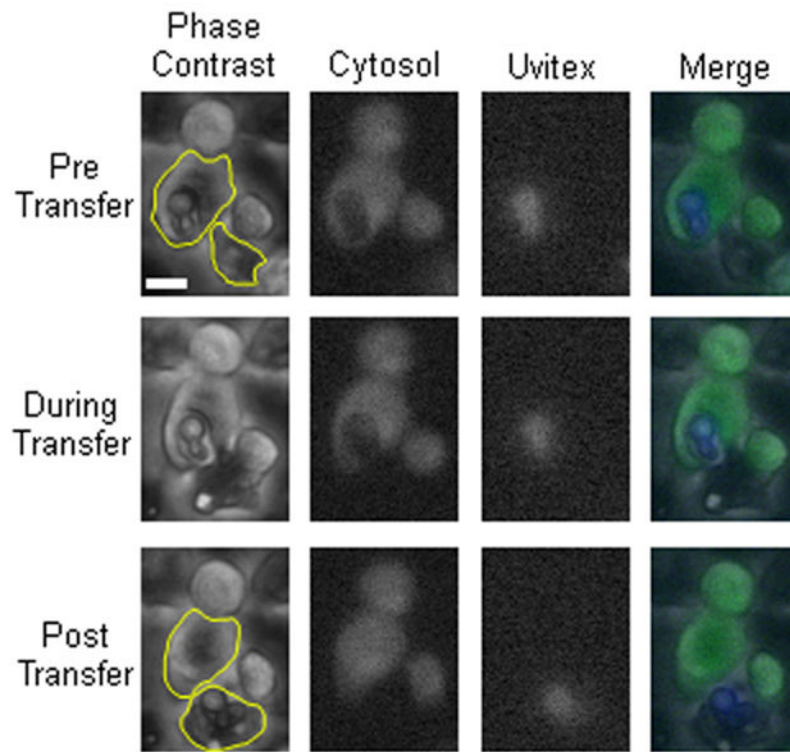


**Figure 1.** Dragocytosis event captured via fluorescent microscopy. Representative frames before (Pre), during, and after (Post) cryptococcal transfer. 10X Phase Contrast, Cytosolic CellTracker Green CMFDA (Green), Uvitex (Blue), and merged channels. The Scale bar represents 10  $\mu\text{m}$  and is constant for all images. Pre, During, and Post Transfer images were obtained from movie frames 266, 274, and 278, respectively. Representative regions of interest have been outlined (yellow) to demonstrate areas analyzed for fluorescence. These images are from Event 4 in subsequent graphs.

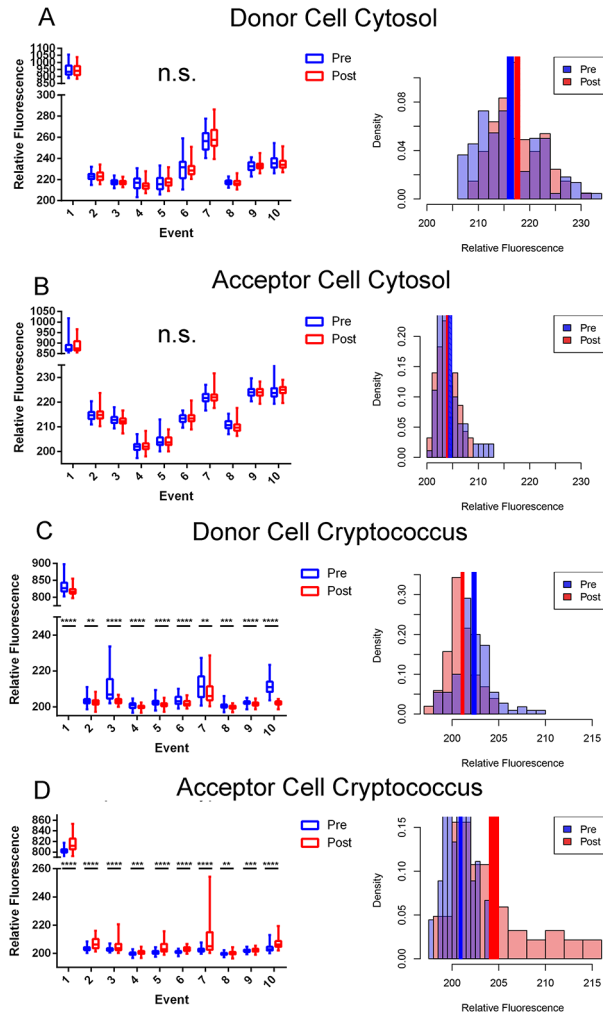


**Figure 2.** Quantifications of stains from Dragotcytosis events in biological replicates. **A.** Donor cell cytosol as measured by CellTracker Green CMFDA intensity before (blue) and after (red) transfer. **B.** Acceptor cell cytosol as measured by CellTracker Green CMFDA intensity before and after transfer. Intensity values remain at background levels in each replicate. **C.** Presence of cryptococcal cell inside Donor cell measured as Uvitex intensity before and after transfer. **D.** Presence of cryptococcal cell inside Acceptor cell measured as Uvitex intensity before and after transfer. Significance was determined by unpaired two tailed *t*-test with (\*\*\*\*) representing a *P* value of < 0.0001, (\*\*\*) representing a *P* value of < 0.001, and (\*\*) representing a *P* value of < 0.01. Data for each population is each individual pixel intensity measurement, with bars representing minimum-maximum spans in box-whisker format. Density (pixel intensity frequency) histograms represent pixel population data specifically for Event 4 with solid colored rectangles representing mean  $\pm$  standard error. Data for each event consists of intensity measurements from each pixel within the acceptor or donor cell. The relative fluorescence of Event 1 is higher than the other events because that measurement came from the initial experiment before dyes were titrated for optimization. Each of these events corresponds to a single event in which a single yeast is

transferred from one macrophage to another with the exception of event 8 which spans two individual transfer events in which one yeast cell is transferred during each event. This was due to the necessity of acquiring clear frames for quantification.

Author Manuscript

Author Manuscript

Author Manuscript

Author Manuscript

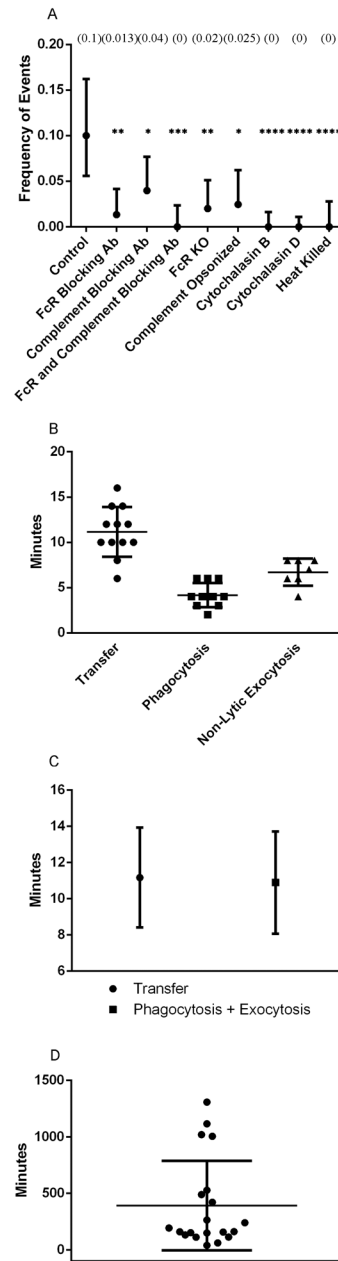


**Figure 3.** Inhibition and timing of transfer events supports exocytosis-phagocytosis hypothesis. **A.** Quantification of the frequency of transfer events observed between BMDMs supplemented with different inhibitor antibody combinations. Frequency values represent frequency of events based on number of events in all infected cells, with complete information found in Table I. *P* values calculated via one tailed proportion test. **B.** Quantification of the total timespan of each transfer event as well as phagocytosis ingestion time determined by total frames captured. **C.** Quantification of the total timespan of transfer events compared to the addition of phagocytosis and exocytosis events. Data points represent population average with bars representing population standard deviations. *P* value calculated as non-significant

via unpaired two tailed *t*-test. **D.** Timespan between the start of an experiment and the initial frame of transfer events. Events began at 392 min post infection (SD +/- 395 min) with most events occurring before 9 h.

Author Manuscript

Author Manuscript

Author Manuscript

Author Manuscript

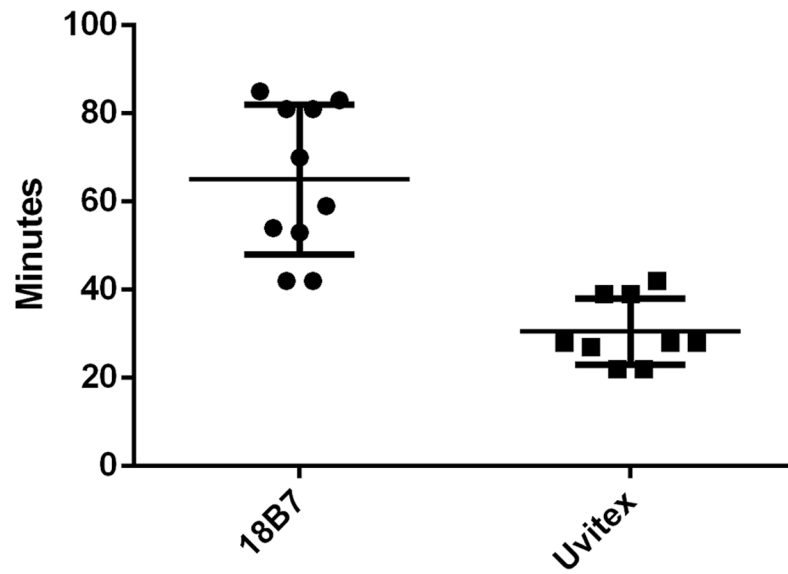


**Figure 4.** Temporal dynamics of dye acquisition for Uvitex 2B and 18B7-Oregon Green in BMDM ingested *C. neoformans*. Quantification of the amount of time, in minutes, required for a cryptococcal cell to be exposed to the extracellular environment in order to acquire a clear dye signal for 18B7-Oregon Green (65 min) and Uvitex 2B (30 min).

Author Manuscript

Author Manuscript

Author Manuscript

Author Manuscript

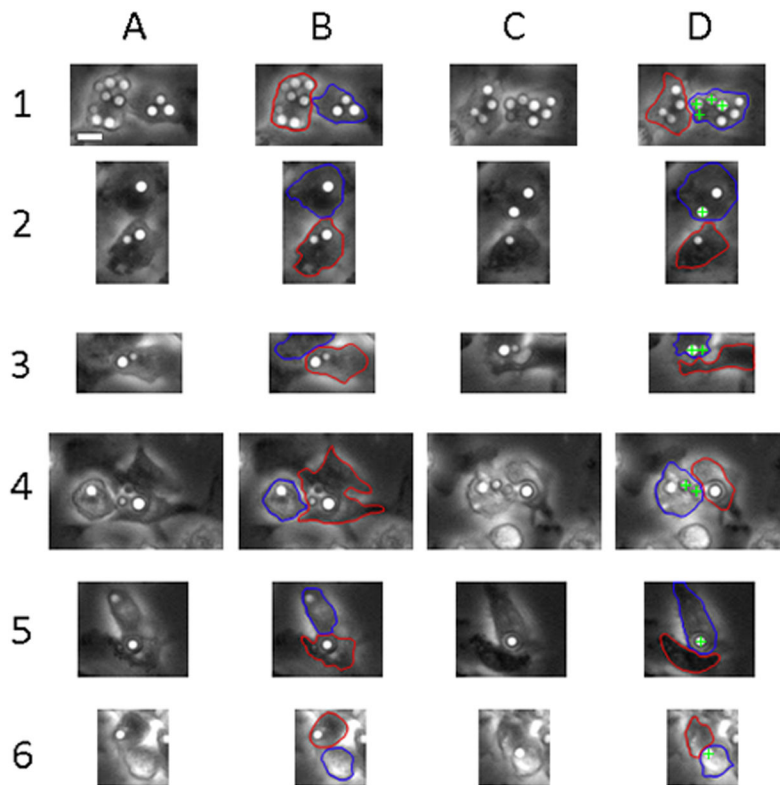


**Figure 5.** Visualization of donor and acceptor macrophages immediately pre- and post-transfer events. **A.** Initial image of donor and acceptor cells immediately prior to transfer. **B.** Initial image pre-transfer with donor (red) and acceptor (blue) cells outlined. **C.** Initial image of donor and acceptor cells immediately after transfer. **D.** Initial image post-transfer with donor (red), acceptor (blue), and transferred crypto (green cross) cells noted. Scale bar represents 10  $\mu\text{m}$  and is consistent throughout images.



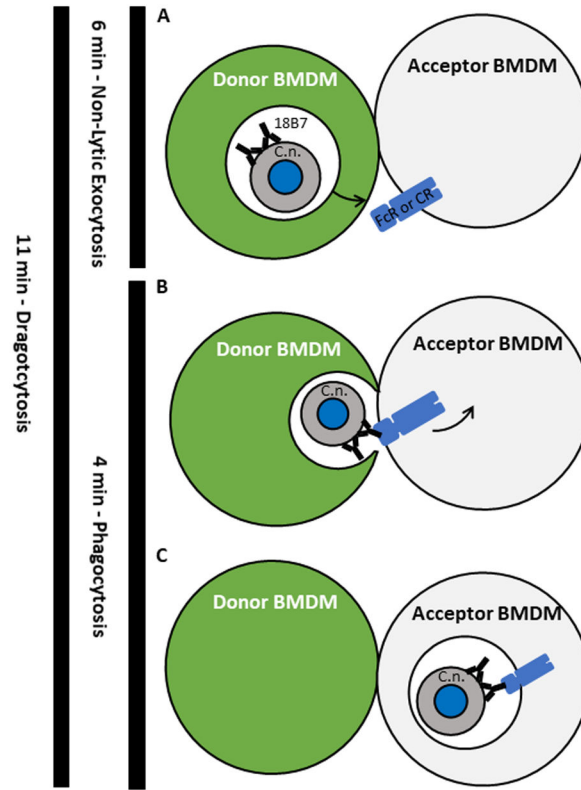


**Figure 6.** Proposed overarching model of cryptococcal cell-to-cell transfer. **A.** The initial step in transfer, and the point which was defined as the start of exocytosis. The moment when a phagosome (white space) containing an opsonized cryptococcal cell begins to move toward the plasma membrane of the donor macrophage. The phagosome reaches and merges with the plasma membrane of the donor macrophage in a manner which expels the cryptococcal cell. Cytosol is retained within the donor macrophage and excluded from the transfer process. The moment at which the cryptococcal cell is fully expelled from a macrophage was defined as the end of exocytosis. **B.** The next step of transfer in which the released cryptococcal cell is free to interact with the Fc receptor of the acceptor macrophage via opsonin which survives the initial phagosome. The moment of initial attachment of the cryptococcal cell to the acceptor macrophage defined as the start of phagocytosis. Note the macrophage cells remain in contact but the transfer site is not sealed to the extracellular environment. **C.** The final step of transfer, the point at which the cryptococcal cell has been fully ingested by the acceptor macrophage. This moment is also used to define the end of phagocytosis. **Left.** The total time of exocytosis, phagocytosis, and Dragocytosis denoted by black line and measured time. The total length of Dragocytosis roughly equals that of exocytosis plus phagocytosis.

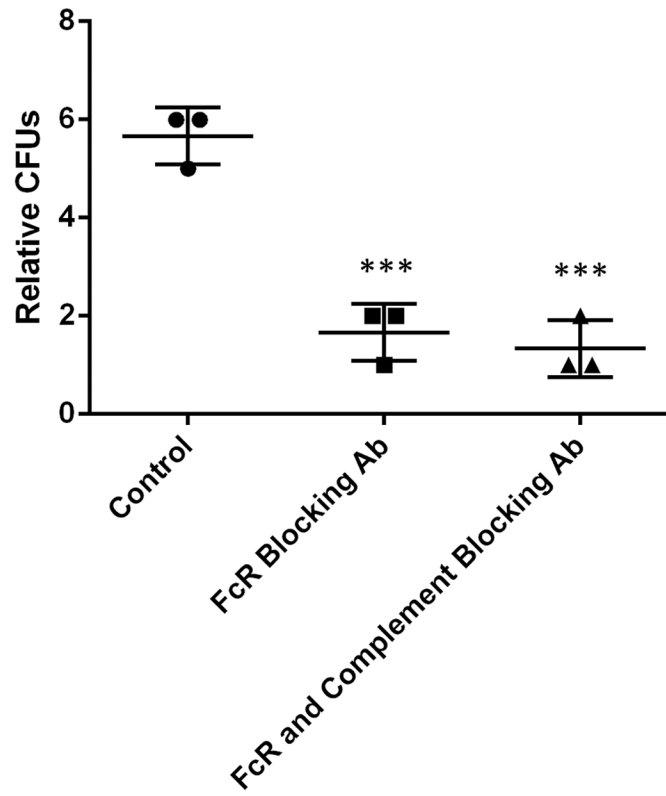


**Figure 7.** Relative quantification of surviving intracellular *C. neoformans*. Fungal colonies were enumerated via serial dilution after a 24 h infection period in which BMDMs were incubated with different combinations of inhibitory antibodies. \*\*\* denotes  $P < 0.001$  compared to control.

**Table I.**

Quantified cellular events in the presence or absence of antibody receptors. Counts are written as “Total # (Percent)”. Lytic exocytosis is denoted as N/A for cytochalasin experiments because the drug results in cell death starting approximately 10 h into the experiment.

Event	Control	aCD16/32	aCD11b	aCD16/32 + aCD11b	FcR KO	Complement Opsonized	Cyto B	Cyto D	Heat Killed
<b>Lytic Exocytosis</b>	12 (6.9)	1 (0.67)	0	1 (0.8)	6 (4.03)	9 (7.38)	N/A	N/A	0
<b>Non-Lytic Exocytosis</b>	9 (5.1)	1 (0.67)	4 (2.65)	1 (0.8)	4 (2.68)	6 (4.92)	0	0	0
<b>Transfer</b>	14 (8)	2 (1.34)	6 (3.97)	0	3 (2.01)	3 (2.50)	0	0	0
<b>Total Infected Cells</b>	140	149	151	126	149	122	221	329	169

**Table II.**

Annotated genes differentially expressed in macrophages incubated with Fc receptor blocking antibody. Samples were compared to macrophages pre-incubation and post-incubation without antibody. Two genes are omitted due to lack of annotation.

GenbankAccession	Symbol	GeneName	p-value	Fold-Change
<a href="#">AK164118</a>	Phyhipl	phytanoyl-CoA hydroxylase interacting protein-like	0.043635	2.49488
<a href="#">NM_009140</a>	Cxcl2	chemokine (C-X-C motif) ligand 2	0.0204045	2.37112
<a href="#">NM_011879</a>	Ik	IK cytokine	0.0417661	2.015
<a href="#">NM_013877</a>	Cabp5	calcium binding protein 5	0.0249099	2.59332
<a href="#">NM_026268</a>	Dusp6	dual specificity phosphatase 6	0.0186441	2.28549
<a href="#">NM_199022</a>	Shc4	SHC (Src homology 2 domain containing) family, member 4	0.047315	2.39855
<a href="#">XM_006500371</a>	Trp53rkb	transformation related protein 53 regulating kinase B	0.0397998	2.39335